Available online at www.sciencedirect.com
SCIENCE DIRECT®
Polymer 44 (2003) 7651–7659
polymer
www.elsevier.com/locate/polymer

Thermo-sensitive poly(*N*-vinylcaprolactam-*co*-acetoacetoxyethyl methacrylate) microgels: 2. Incorporation of polypyrrole

Andrij Pich[a,*], Yan Lu[a], Volodymyr Boyko[b], Karl-Friedrich Arndt[b], Hans-Juergen P. Adler[a]

[a]*Institute of Macromolecular Chemistry and Textile Chemistry, Dresden University of Technology, D-01062 Dresden, Germany*
[b]*Institute of Physical Chemistry and Electrochemistry, Dresden University of Technology, D-01062 Dresden, Germany*

Received 24 March 2003; received in revised form 18 August 2003; accepted 11 September 2003

Abstract

In a previous paper [Polymer (2003) in press DOI: 10.1016/j.polymer.2003.09.037] polymeric temperature-sensitive microgels were prepared by surfactant-free emulsion co-polymerization of *N*-vinylcaprolactam (VCL) and acetoacetoxyethyl methacrylate (AAEM). In the present work, VCL/AAEM microgels were used as a template for oxidative polymerization of pyrrole (Py). It was found that pyrrole polymerization takes place directly in microgel structure leading to composite particles. Influence of microgel structure and amount of incorporated polypyrrole (PPy) on particle properties is discussed. Obtained stable composite microgels show similar thermal sensitivity as VCL/AAEM particles with fully reversible collapse-swelling properties.

Keywords: Microgel; Polypyrrole; Swelling

1. Introduction

During the last decade conductive polymers have received increased interest both for academic purposes and for potential applications. One of the important areas of research on conducting polymers concerns methods for making them processable. The main approaches can be divided into three main groups: (1) preparation of composites with other polymers, (2) synthesizing of soluble derivatives, and (3) synthesis of dispersions of insoluble conducting polymers. Synthesis of polymeric dispersions requires the selection of an appropriate stabilizer to provide the effective stabilization of colloidal system and to control the morphology and size of polymer particles.

Recently, there have been reports of the successful production of PPy and polyaniline (PANI) latex particles by chemical oxidation in either water or other media in presence of different stabilizers. Stabilizers can be divided into the following groups: surfactants; water-soluble functional polymers; inorganic colloids; and polymer latexes.

The first PANI dispersion stabilized with an anionic surfactant dodecylbenzenesulfonic acid (DBSA) was prepared by DeArmitt and Armes [2]. The surfactant-stabilized PPy particles were produced by the oxidation of pyrrole with sodium persulfate in the solution of sodium dodecylbenzene sulfonate [2,3].

The water-soluble polymers used as stabilizers were poly(vinylpyrrolidone) (PVP) and poly(vinyl alcohol-co-acetate) (PVA) [4,5], poly(ethyleneoxide) (PEO) [6], poly(2-vinyl pyridine-co-butyl methacrylate) (P2VP-BM) [7], poly(*N*,*N*′-dimethylaminoethyl methacrylate-b-n-butyl methacrylate) [8], poly(vinyl acetate) [9], poly(vinyl methyl ether) (PVME) [10], ethylhydroxycellulose (EHEC) [11,12], poly(2-(dimethylamino)ethylmethacrylate-*stat*-3-vinylthiophene) [13], poly(styrenesulfonate) (PSS) [14] etc.

Ultrafine colloidal silica of 7 and 22 nm has been used for the first time for the stabilization of PANI colloids by Gill et al. [15,16]. Early experiments have shown that, besides silica, tin(IV) oxide [17], manganese(IV) oxide and zirkonium dioxide [18,19] were also effective stabilizers for PPy, PANI and poly(*N*-vinylcarbazole) colloids.

Utilizing potential features of polymer latexes as stabilizers Beadle et al. [20] polymerized aniline in the presence of chlorinated latex of 200 nm size. Liu et al. [21] used polystyrene particles functionalized by sulfonic and

* Corresponding authors.
E-mail addresses: andrij.pich@chemie.tu-dresden.de (A. Pich).

0032-3861/$ - see front matter © 2003 Elsevier Ltd. All rights reserved.
doi:10.1016/j.polymer.2003.09.038

carboxylic groups for modification with PPy and no colloidal destabilization was observed.

The confined polymerization of conducting polymers is a very pertinent way to give them controlled shape and dimension, which addresses the question of the availability of appropriate templates. The use of microtubules of PPy rather than films is much more efficient for the immobilization of biologically active species such as glucose oxidase and, in this case, for the direct electron transfer between the enzyme and the conducting polymer, so improving the electrochemical detection [22]. Martin et al. [23–26] used commercially available particle track-etched membranes (PTM's) as templates for the preparation of nanofibrils of metals, semiconductors, and conducting polymers. They focused on the synthesis of three conducting polymers, namely polypyrrole, poly(3-methylthiophene), and polyaniline, within the pores of a polycarbonate (PC) Nucleopore membrane. Recently, Demoustier-Champagne et al. [27–30] reported on the use of these nanoporous PTM's as templates for the chemical and electrochemical synthesis of nanoshaped conducting polypyrrole nanostructures. Jerome et al. [31] reported synthesis of PPy nanowires by two-step electrochemical process where the poly(ethyl acrylate) grafted onto carbon electrode served as a template. These authors found that the solvent used for pyrrole polymerization had a strong influence on the polymer morphology. PPy wires were formed in dipolar aprotic solvents (DMF or DMSO), whereas the more traditional cauliflower-like morphology was observed in less polar solvents (acetonitrile, ACN) [32]. Wan et al. [33] created a template-free method to synthesize microtubules of PANI [34] and PPy [35] in the presence of β-naphthalene sulfonic acid (β-NSA) micelles. Compared with the methods mentioned previously, the template-free method is not so costly and rather more simple.

The idea behind this work was to prepare 'smart' polymer sub-micron particles containing conjugated polymer. In the present paper we describe the synthesis of composite polypyrrole particles in the presence of thermosensitive poly (vinyl caprolactam-acetoacetoxyethyl methacrylate) (VCL/AAEM) microgels that, as expected, should play the roles of both template and stabilizer. The synthesis and characterization of VCL/AAEM microgels are explained in details elsewhere [1]. The chemical structure of VCL/AAEM co-polymer is presented in Scheme 1.

Thermosensitive microgels based on VCL and AAEM have been prepared in surfactant free conditions. Overall VCL/AAEM ratio determines size of microgels below LCST due to regulation of crosslinking and at low temperatures particles swell to different extent. It has been assumed that the microgels have core-shell structure due to fast consumption of more reactive methacrylic monomer in the beginning of reaction. AAEM-rich particle core is more hydrophobic and is less temperature sensitive if to compare with VCL-rich shell. VCL/AAEM microgel particles exhibit completely reversible 'soft-hard sphere' transition

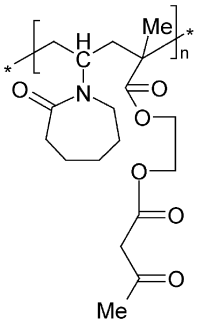

Scheme 1. Chemical structure of VCL/AAEM copolymer.

induced by collapse of highly swollen VCL-rich shell during heating. The polymerization of pyrrole in presence of VCL/AAEM microgels can result in novel composite microgels filled with conducting polypyrrole inclusions and additionally possessing thermo-sensitive properties.

2. Experimental

2.1. Materials

Acetoacetoxyethyl methacrylate was obtained from Aldrich and purified by conventional methods and then vacuum distilled under nitrogen. *N*-vinylcaprolactam was obtained from Aldrich and purified by distillation. Initiator, 2,2′-azobis(2-methylpropioamidine) dihydrochloride (AMPA) was obtained from Aldrich and used as received. Deionized water was employed as polymerization medium. Cross-linker *N*,*N*′-methylenebisacrylamide (MBA) from Aldrich was used without further purification. Pyrrole (Py) was purchased from Aldrich, distilled under vacuum, and stored in a refrigerator before use. Sodium peroxydisulfate (SPDS) was obtained from Aldrich and used as received. Deionized water was employed as polymerization medium.

2.2. VCL/AAEM microgels

Appropriate amounts of AAEM, VCL (see Table 1) and 0.06 g of cross-linker (3 mol%) were added in 145 ml deionized water. Double-wall glass reactor equipped with stirrer and reflux condenser was purged with nitrogen. Solution of the monomers was placed into reactor and stirred for 1 h at 70 °C with purging with nitrogen. After

Table 1
Composition and some properties of VCL/AAEM microgels

Run	VCL (g)	AAEM (g)	AAEM[a] (mol%)	Solids (%)	pH
1	2.06	0.04	4.3	1.2	7.1
2	2.04	0.08	4.8	1.2	7.0
3	1.98	0.16	6.7	1.2	7.2
4	1.93	0.24	11.8	1.2	7.1
5	1.88	0.32	15.2	1.2	7.1

[a] Determined by elementary analysis.

that, the 5 ml water solution of initiator (5 g/l) was added under continuous stirring. Reaction was carried out for 8 h. The polymerization yield, determined gravimetrically, was around 80%. Some important characteristics of microgels used in this study are summarized in Table 1.

2.3. Polymerization of pyrrole

VCL/AAEM microgel was diluted with appropriate amount of water at 25 °C in reactor equipped with stirrer. Then the pyrrole was added to the stirred solution and reactor was purged with nitrogen for 15 min. Oxidant was dissolved in water in separate flask and added to the reaction mixture to start the polymerization. Polymerization was allowed to proceed for 10 h.

2.4. Cleaning procedure

Polymer dispersions were freed from monomer by dialysis. Latexes were dialysed against water using Millipore Amicon Miniplate membrane (MWCO-10000).

2.5. IR-Spectroscopy

IR spectra were recorded with Mattson Instruments Research Series 1 FTIR spectrometer. Dried polymer samples were mixed with KBr and pressed to form a tablet.

2.6. Particle size analysis

In dynamic LLS, the intensity–intensity–time correlation function $g_2(q,t)$ in the self-beating mode was measured and can be expressed by the Siegert relation:

$$g_2(q,t) = A(1 + \beta|g_1(q,t)|^2) \quad (1)$$

where t is the decay time, A is a measured baseline, β is the coherence factor, and $g_1(q,t)$ is the normalized first-order electric field time correlation function and $g_1(q,t)$ is related to the measured relaxation rate Γ:

$$g_1(q,t) = \exp(-\Gamma t) = \int G(\Gamma)\exp(-\Gamma t)\mathrm{d}\Gamma \quad (2)$$

A line-width distribution $G(\Gamma)$ can be obtained from the Laplace inversion of $g_1(t)$ (CONTIN procedure) [10]. For a pure diffusive relaxation, Γ is related to the translational diffusion coefficient D at $q \rightarrow 0$ and $c \rightarrow 0$ by

$$D = \Gamma/q^2 \quad (3)$$

or a hydrodynamic radius R_h given by

$$R_h = k_B T/(6\pi\eta D) \quad (4)$$

with q, k_B, T and η being scattering vector, the Boltzmann constant, absolute temperature, and solvent viscosity, respectively. All DLS experiments were carried out at angles $\theta = 30–140°$. The concentration of the microgel in water was about 1.5×10^{-5} g/ml. Microgel solutions were filtrated using 5 μm nylon filters. Typically, the sample in a 10 mm test tube was immersed in a toluene bath and thermostated within an error of ±0.1 °C.

Typically, three measurements were performed for determination of the radius of gyration and five for the hydrodynamic radius. Accuracy of measurements for hydrodynamic radius is ±3%.

2.7. Scanning electron microscopy

SEM images were taken with Gemini microscope (Zeiss, Germany). Samples were prepared in the following manner. Dispersions were diluted with deionized water, dropped onto aluminium support and dried at room temperature. Pictures were taken at voltage of 4 kV.

3. Results and discussion

VCL/AAEM microgel particles have been used as templates for oxidative polymerization of pyrrole. Fig. 1 shows schematically the incorporation of polypyrrole into microgels.

In the first step (1) pyrrole was added to microgel dispersion. Since pyrrole has limited solubility in water, it can be assumed that some amount of monomer is solubilized in hydrophobic domains of microgel network. In the second step (2) the addition of oxidant (sodium peroxydisulfate, SPDS) starts oxidative polymerization of pyrrole in the system. At this stage two possible scenario can be considered: (a) incorporation of polypyrrole (PPy) particles into microgel structure and formation of composite particles without strong change in polydispersity of the system; and (b) partial incorporation of PPy into microgels and formation of secondary PPy particles, which are not deposited into microgel network. Naturally, scenario (a) is preferable since such system is easy to handle and more suitable for future applications. Additionally, since VCL/AAEM microgels are thermo-sensitive and collapse when solution is warmed up (LCST around 28 °C) it is expected that composite microgels will also show thermo-sensitive properties to some extent

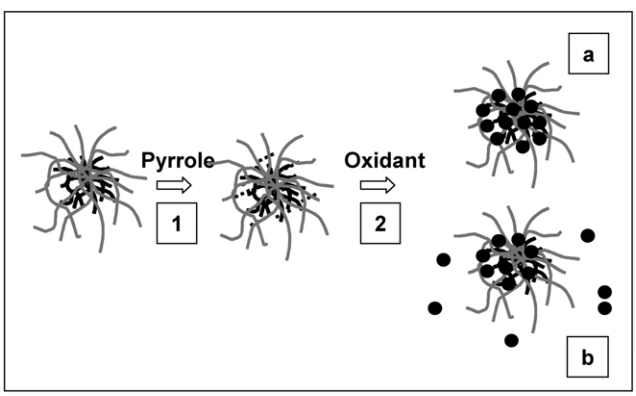

Fig. 1. Polymerization of pyrrole in presence of AAEM/VCL microgels.

Table 2
Reaction recipes for preparation of composite microgels

Run	AAEM (mol%)	Microgel solution (g)	Py (g)	Water (g)	SPDS (g)	T^r (°C)	PPy^T (%)	PPy^a (%)	Conversion (%)
6	4.3	40	0.05	5	0.25	20	9.43	7.58	80.4
7	4.8	40	0.05	5	0.25	20	9.43	8.68	92.1
8	6.7	40	0.05	5	0.25	20	9.43	5.54	58.8
9	11.8	40	0.05	5	0.25	20	9.43	6.55	69.5
10	15.2	40	0.05	5	0.25	20	9.43	7.39	78.4

Amount of sulfate was determined by elementary analysis.
[a] Amount of polypyrrole.

combining this interesting feature with conductivity provided by PPy inclusions.

3.1. Influence of AAEM content

The amounts of reagents used for polymerization of pyrrole in presence of VCL/AAEM microgels are summarized in Table 2.

In this first set of experiments equal pyrrole amounts were added to microgel solution in every reaction run. The amount of PPy incorporated into microgels was determined by elementary analysis. Results presented in Table 2 indicate that microgels contain around 6–7% PPy (theoretical value was 9.4%). Fig. 2. shows the average hydrodynamic radius (R_h) of VCL/AAEM microgels and their composite analogues.

It is clear from Fig. 2 that incorporation of large amounts of AAEM into microgel structure reduces the particle size. This behaviour is not surprising since effective steric stabilization at room temperature arises from VCL segments, which probably form a hairy layer around particles. Increase of AAEM content leads to increased tendency of crosslinking reactions and more defined heterogeneity of the particles due to large difference in reactivity of VCL and AAEM [1]. Fig. 2 indicates that composite microgels with integrated polypyrrole domains are considerably smaller than original particles. Incorporation of pyrrole causes the

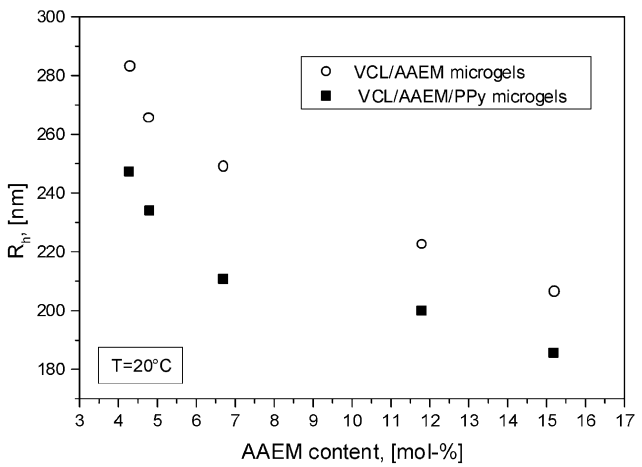

Fig. 2. Average hydrodynamic radius of microgels as a function of AAEM content.

shrinkage of the microgel network probably due to the interaction between polypyrrole domains and polymer network. In this case it is possible to assume that the carbonyl functions of AAEM units will form hydrogen bonds with nitrogen atoms of pyrrole rings. Similar kind of interactions was observed by Armes et al. [7] for polypyrrole particles stabilized by poly(2-vinyl pyridine-co-butyl methacrylate) steric stabilizers. In all cases DLS spectra were monomodal and no broadening of particle size distribution was detected after pyrrole polymerization. This indicates that polypyrrole domains are located in microgel network and these microgels can be considered as effective templates. Additional proof for that is presented in Fig. 3. In this case in run 9 the pyrrole polymerization process was followed by DLS measurements.

Fig. 3 indicates that hydrodynamic radius decreases continuously from the beginning of polymerization and finally reaches the plateau after 100 min. It is also evident that the particle size distribution remains without strong changes and no separate polypyrrole particles in water medium were detected. Therefore, microgel network can be considered as polymerization loci in present system.

The particle size of obtained microgels was also measured at different temperatures. Fig. 4(a) indicates that the size of VCL/AAEM microgels decreases with increasing temperature. This typical LCST behaviour was detected also from composite microgels (Fig. 4(b)).

The deswelling process for both systems takes place in the same temperature region, but the shrinkage of pyrrole-containing particles represented as the ratio of average hydrodynamic radii at 10 and 45 °C (R_h^{10}/R_h^{45}) is smaller (see also Table 3). This indicates that PPy inclusions interact with microgel network and this leads to decrease of

Table 3
Thermal shrinkage of the VCL/AAEM (run 1–6) and VCL/AAEM/PPy (run 6–8) microgels

Run	R_h^{10} (nm)	R_h^{45} (nm)	R_h^{10}/R_h^{45}
1	308	137	2.25
3	269	124	2.17
5	219	130	1.68
6	253.5	119.7	2.12
8	233.5	127.8	1.83
10	206.8	123.3	1.67

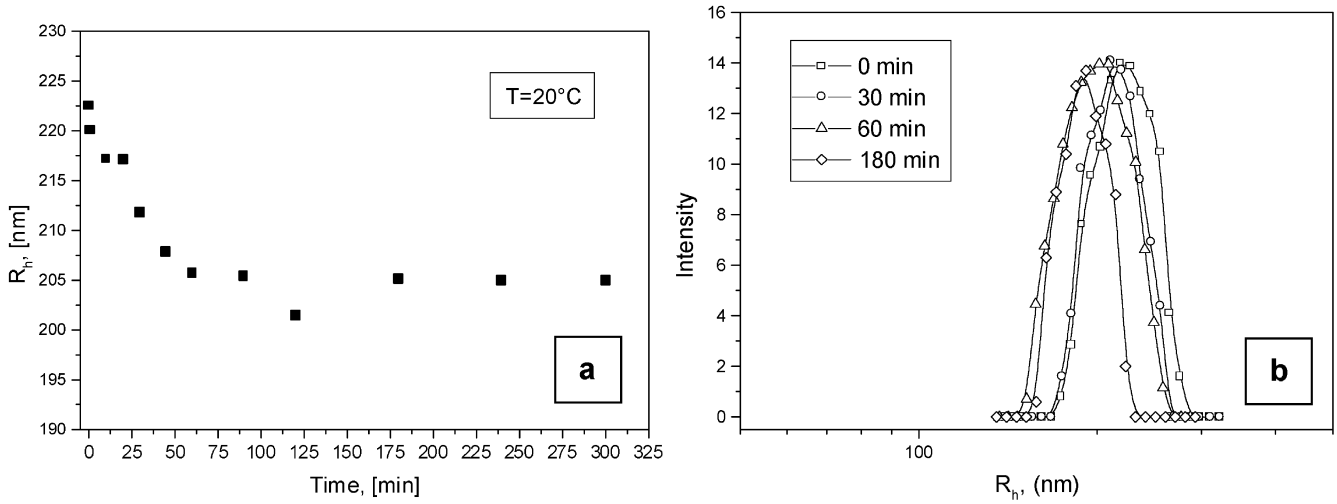

Fig. 3. Average hydrodynamic radius (a) and particle size distribution of the composite particles (b) as a function of reaction time (run 9: microgel with 11.8 mol% AAEM).

microgel size at temperatures below LCST. It can be assumed that PPy chains form hydrogen bonds with nitrogen atoms of VCL. For samples with highest AAEM content the ratio R_h^{10}/R_h^{45} is nearly the same for both VCL/AAEM and VCL/AAEM/PPy particles, which is probably due to higher crosslinking density of the microgel template.

Both VCL/AAEM and corresponding composite particles collapse to the same size and this indicates that the pyrrole amount incorporated in microgel structure is not sufficient to form the IPN-structure. So, polypyrrole inclusions do not disturb the deswelling process. It is also surprising that charged polypyrrole particles do not influence the collapse temperature of microgels.

3.2. Influence of PPy content

In this set of experiments microgel prepared at 4.8 mol% AAEM content (run 2) was used and the pyrrole concentration was varied. Table 4 presents the amounts of ingredients used in these reactions.

Experimental results of particle size measurements for obtained composite microgels are presented in Fig. 5(a). When the oxidant was added to the VCL/AAEM microgel and Py was not present in reaction mixture the average hydrodynamic radius of particles slightly decreases. It is well known, that hydrogels exhibit different equilibrium degrees of swelling in response to various kinds of salts as well as their concentrations. Donnan equilibrium has been successfully used to predict the swelling behaviour of charged gels in electrolyte solutions [36–38]. In the case of non-ionic gels, increased salt concentration in the bulk medium affects inter- and intramolecular hydrogen-bonding and polar interactions as well as hydrophobic interactions associated with water molecules. Thus, it can be anticipated that, even though non-ionic gels demonstrate the salting-out (or salting-in) behaviour, they normally induce a far weaker salt-induced swelling change compared to the ionic gels.

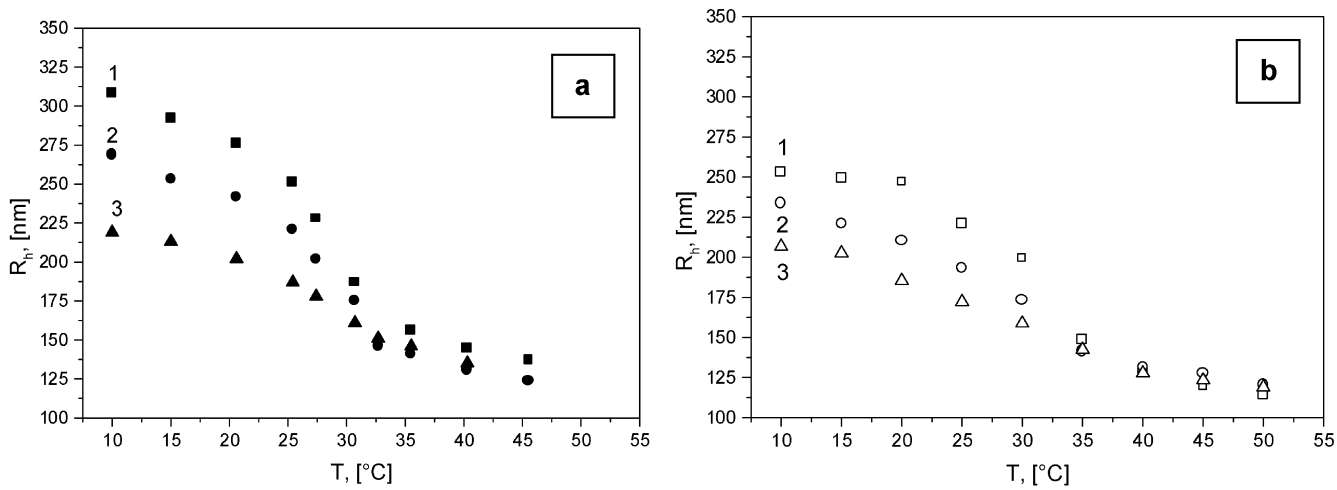

Fig. 4. Average hydrodynamic radius of AAEM/VCL microgels (a) (1—run 1; 2—run 3; 3—run 5) and composite microgels (b) (1—run 6; 2—run 8; 3—run 10) as a function of the temperature.

Table 4
Reaction recipes for preparation of composite microgels with different PPy content

Run	Microgel solution[a] (g)	Py (g)	Water (g)	SPDS (g)	T^r (°C)	Ppy^T (%)	PPy^b (%)	Conversion (%)
11	40	0.025	5	0.125	20	4.95	3.04	61.4
12	40	0.04	5	0.20	20	7.69	4.07	52.9
13	40	0.05	5	0.25	20	9.43	8.68	92.1
14	40	0.065	5	0.325	20	11.93	9.77	81.9
15	40	0.08	5	0.40	20	14.29	14.23	99.6
16	40	0.1	5	0.50	20	16.67	16.33	97.9

[a] Run 2: 4.8 mol% AAEM.
[b] Determined by elementary analysis.

According to an empirical equation of the salting-out, the solubility of any particular water-soluble polymer decreases gradually with increasing ionic strength. Kirsh et al. [39] investigated influence of different salts on transition temperature of PVCL. Mostly linear decrease of LCST with increasing salt concentration was detected for different anions, and the coefficient of stabilization for sulfate was found to be minimal among tested salts. Park et al. [40] reported that different salts lower the LCST of non-ionic poly(*N*-isopropylamide) gel with increasing concentration. In this case it could be proposed that adding salt in non-ionic microgels would affect Flory interaction parameter for the polymer chains with the solvent molecules, which consequently results in a decrease of LCST. VCL/AAEM microgel is not an example of charged system, however, some charges from initiator molecules incorporated into microgel network cannot be neglected. Probably, oxidant molecules shift the LCST to lower temperatures and particles dimensions decrease at 20 °C as it is shown in Fig. 5(a).

The average hydrodynamic radius of microgels decreases much strongly when the PPy content increases and when the minimal value is reached particle size starts to increase. Fig. 5(b) indicates that there was no strong changes in particle size distribution, so this effect cannot be caused by presence of small PPy particles beside large composites (arrows in Fig. 4(a) indicate the samples measured by DLS presented in Fig. 5(b)). When the PPy content was higher than 16% system became unstable.

Initial decrease of the particle size can be explained by some specific interaction of polypyrrole domains and polymer network. When the PPy amount is low filler particles are located with certain distance from each other and the VCL/AAEM polymer chains can interact effectively with polypyrrole particle surface. So, stepwise increase of the PPy particles content leads to the shrinkage of the microgel template. This situation is possible up to certain content of PPy particles in microgel structure. If PPy content reaches certain value, the distance between inclusions will be smaller. Therefore, the repulsion forces between charged polypyrrole filler particles will dominate and the size of composite microgel increases with further increase of PPy content.

Fig. 6 presents the R_h^{10}/R_h^{45} ratio for composite microgels (runs 11–16) plotted against PPy contents in microgel structure. This dependency is quite similar to the behaviour of hydrodynamic radius in Fig. 5(a). It was found that microgels prepared with different PPy contents collapse nearly to the same size, but swell to different extent at lower temperatures. Therefore, dependency in Fig. 5 is determined actually by change of the size of microgels in swollen state.

From this it can be concluded, that if the template is in

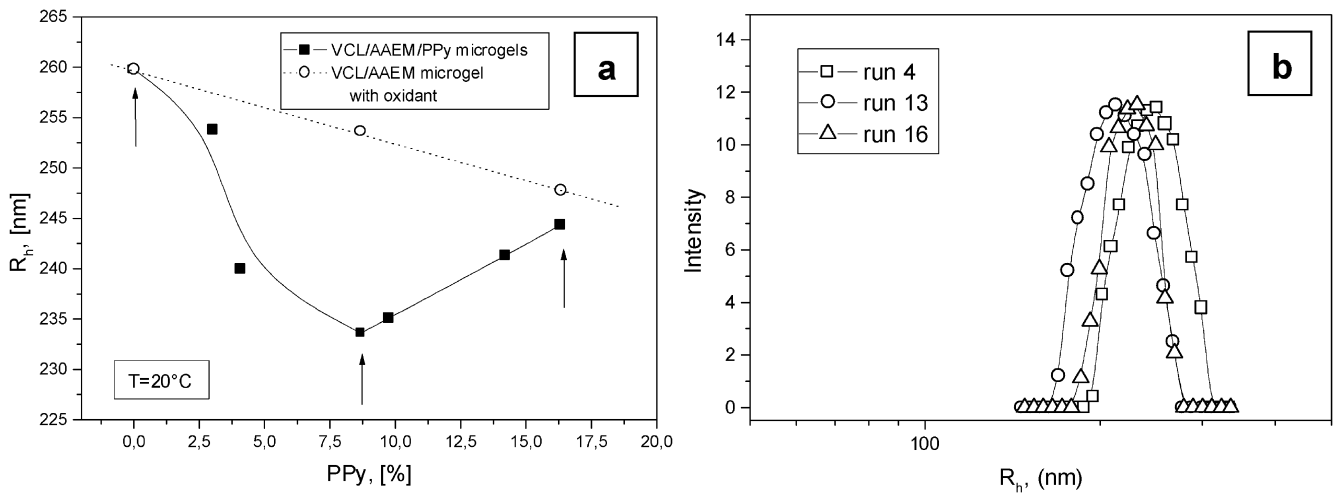

Fig. 5. Average hydrodynamic radius (a) and particle size distribution (b) of composite microgels as a function of PPy content.

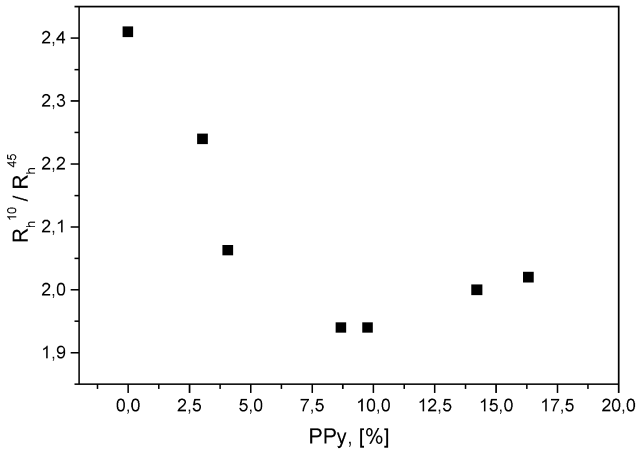

Fig. 6. R_h^{10}/R_h^{45} ratio as a function of PPy content.

swollen state (low temperatures) the polypyrrole inclusions affect the microgel size by combination of attraction/repulsion forces. Contrary, at high temperatures, the dimensions of composite microgels are determined exclusively by the shrinkage of VCL/AAEM network.

It was already mentioned that at certain polypyrrole content microgel particles are loosing stability in water. This fact is not surprising, since according to the idea described before, at high concentration of PPy particles the surface of composite microgels will be totally covered by filler particles. This can cause compression of the hydrophilic hairy layer of microgels responsible for stabilization of the particles with next flock formation or total destabilization of colloidal system.

The modification of VCL/AAEM particles with polypyrrole was confirmed by IR spectroscopy. In Fig. 7 the IR spectra of chemically prepared PPy, VCL/AAEM copolymer (11.8% AAEM) and same VCL/AAEM modified with 16.33% PPy are shown. Major changes can be observed in the region 1500–400 cm^{-1}. The spectrum of VCL/AAEM/PPy composite represents a superposition spectrum of pure components. The ν_{ring} vibration of PPy at 1558 cm^{-1} is overlapped by strong C=O signals of both VCL and AAEM and not shown in Fig. 7. Other characteristic polypyrrole signals such as δ(C–H) (m) at 1037 cm^{-1}; δ(C–H) out of plane (s) at 910 cm^{-1}; and γ(C–H) (w) at 672 cm^{-1} are marked with the arrows.

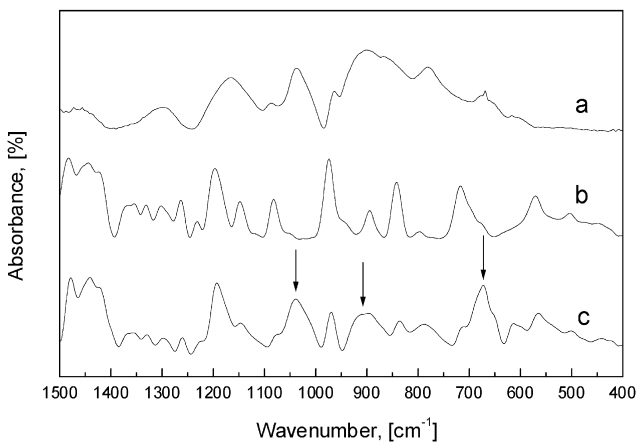

Fig. 7. IR spectra of (a) pure PPy, (b) VCL/AAEM copolymer (run 4), and (c) VCL/AAEM/PPy composite (run 16).

The variation of ξ-potential of the microgel particles without PPy and composite particles with different amounts of loaded PPy are shown in Fig. 8. In the entire pH range, from 1.0 to 10 the ξ-potential for VCL/AAEM microgel particles is positive owing to presence of positively charged groups of initiator residue incorporated into the polymer chains during polymerization process. However, one can see that measured ξ-potential values are very small indicating that VCL/AAEM microgels in swollen state are stabilized not by electrostatic mechanism. Good solubility of VCL-rich microgel shell in water at measurement conditions (20 °C) provides efficient sterical stabilization, and some positive charges probably just improve to some extent stability in water.

Incorporation of PPy into microgels induces visible changes in ξ-potential behaviour. Particle charge becomes negative when pH value is larger than 4.5 for composite particles with higher PPy load. Isoelectric point is clearly observed for both samples with loaded 13.1 and 6.2% PPy. Previous investigations in order to investigate ξ-potential of composite PPy particles stabilized by inorganic oxide nanoparticles [41] or polyacrylate lattices [42] resulted in conclusion that both isoelectric points and ξ-potentials of such nanocomposite particles are governed by the nature of the charged groups at the stabilizer particle surface rather than by the conducting polymer component. Markham et al. [43] reported that when PPy particles were prepared with PEO stabilizer it was possible to strip PEO chains from the PPy surface. In this case bare PPy particles prepared with $FeCl_3$ or $(NH_4)_2S_2O_8$ exhibit isoelectric points (8.5 and 6, respectively), so this correlates to some extent with our result presented in Fig. 8. The charging mechanism for PPy

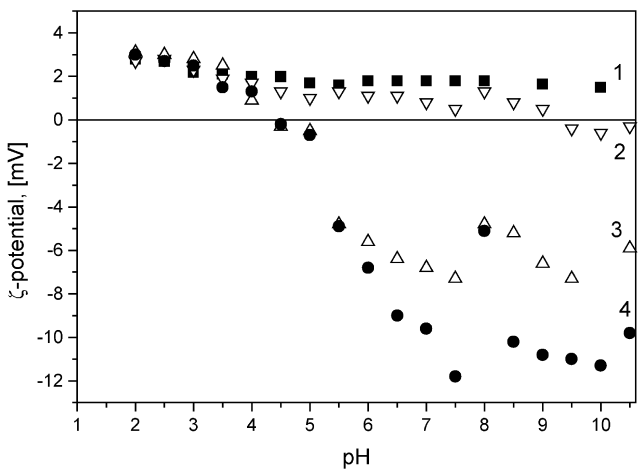

Fig. 8. Variation of the ξ-potential of microgel (run 3) (1) and corresponding composite microgels filled with 5.2% (2), 13.1% (3), and 28.2% PPy (4).

Table 5
Composite microgels prepared at different temperatures

Run	AAEM (mol%)	Py (g)	T^r (°C)	PPy^T (%)	PPy^a (%)	Conversion (%)	Stab	R_h^{10} (nm)	R_h^{45} (nm)	R_h^{10}/R_h^{45}
17	11.8	0.05	30	9.43	9.04	95.9	–	–	–	–
9	11.8	0.05	20	9.43	6.55	69.5	+	212.7	122.0	1.74
18	11.8	0.05	10	9.43	5.64	59.8	+	215.9	125.6	1.72
19	4.8	0.1	30	16.67	16.60	99.6	–	–	–	–
16	4.8	0.1	20	16.67	16.33	97.9	+	260.5	142.7	2.02
20	4.8	0.1	10	16.67	15.87	95.2	+	261.8	144.5	1.81

+, Stable; –, unstable.
[a] Determined by elementary analysis.

is probably a combination of the bulk charge on the polypyrrole chains, arising from oxidation of the pyrrole rings and surface charging possibly due to protonation/deprotonation of the secondary amino groups exposed to the aqueous environment [42]. ξ-potential values measured for composite microgels are probably influenced by the localization of PPy inclusions in the microgel network. We believe that when composite microgel particle is in swollen state PPy domains are not really located on the surface, but embedded into VCL-rich shell. Therefore the effect which we measure is actually a result of the charge compensation of bare PPy particles and microgel network.

Electron microscopy image of composite microgels is shown in Fig. 9. Microgel particles in this SEM picture are in dried state, so the diameter is nearly two times less than measured by DLS in water solution due to the shrinkage of the VCL/AAEM polymer network. The morphology of the composite particles is quite interesting: small polypyrrole domains are incorporated into microgel network, which acts as support for this complicated structure providing spherical shape for whole composite.

It can also be seen that if microgel is in deswollen state polypyrrole inclusions touch with each other. Probably, in water solution the situation is different and polypyrrole particles are separated by highly swollen polymer chains of the microgel template.

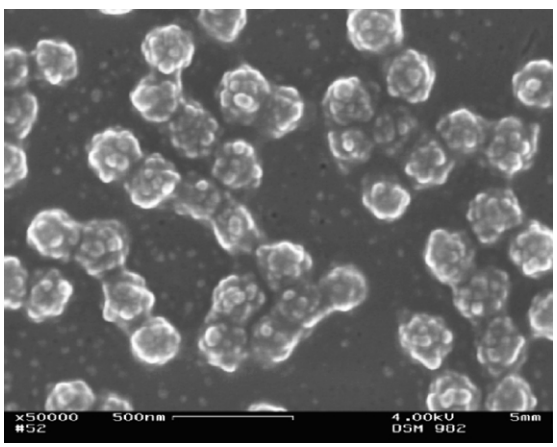

Fig. 9. SEM image of composite microgels filled with 16.33% PPy (run 16).

3.3. Influence of the reaction temperature

Selected pyrrole polymerizations were also performed at different temperatures. It is expected that at different reaction temperatures microgel template will be in different swelling state: lower temperature will induce swelling of the microgel and higher temperature will provide contraction of the network. In this way, the particle number remains constant, but the effective surface area and the porosity of the microgel template can be changed. For this set of experiments microgels containing 4.8 and 11.8 mol% AAEM (runs 2 and 4, respectively) were selected and the pyrrole concentration was constant (see Table 5). Reactions were performed at 10, 20 and 30 °C. Table 5 indicates that experiments performed at 30 °C failed independently on microgel composition and pyrrole amount used. Obtained dispersions were unstable and precipitated immediately when oxidant was added and pyrrole polymerization took place. Colloid stability depends upon the balance of van der Waals attraction, which causes aggregation, and steric or electrostatic forces that oppose aggregation. Below LCST VCL/AAEM microgels are swollen and polymer tails extend from the microgel structure to act as steric stabilizers enhancing colloidal stability. At elevated temperatures the water content of the microgels is reduced to give a higher density and thus a greater Hamaker constant than that at low temperature. Above LCST polymer tails on the microgel surface will be collapsed and thus not contribute to colloidal stability. The electrical charges, which originate from the ionic free radical initiator can play more dominant role in stabilization of colloidal system. Addition of electrolyte induces the compression of double layer and coagulation of VCL/AAEM microgels takes place.

Results of particle size shrinkage for samples prepared at different temperatures presented in Table 5 indicate no significant difference. It seems that the swelling degree of the VCL/AAEM template during pyrrole polymerization has no strong influence on particle size and temperature-induced contraction of composite particles.

4. Conclusions

VCL/AAEM microgels were used as a template for oxidative polymerization of pyrrole. Different PPy amounts have been incorporated into microgel structure. It was found that pyrrole polymerization takes place directly in microgel network leading to formation of composite particles. It seems, that PPy particles interact strongly with VCL/AAEM network and this leads to the change of microgel diameter if the filler content increases. Obtained stable composite microgels show similar thermal sensitivity as VCL/AAEM particles with fully reversible collapse-swelling properties.

Acknowledgements

The authors are thankful to Mrs E. Kern for SEM measurements; Mrs M. Dziewiencki for IR-spectroscopy measurements; Deutsche Forschungsgemeinschaft (DFG, Sonderforschungbereich 287 'Reactive Polymers') and European Graduate School 'Advanced Polymer Materials' (EGK 720-1, DFG) for financial support.

References

[1] Boyko V, Pich A, Richter S, Arndt KF, Adler HJ. Thermo-sensitive poly(*N*-vinylcaprolactam-*co*-acetoacetoxyethyl methacrylate) microgels: 1. Synthesis and characterization. Polymer 2003; DOI:10.1016/j.polymer.2003.09.037 in press.
[2] DeArmitt C, Armes SP. Langmuir 1993;9:652.
[3] Luk SY, Lineton W, Keane M, DeArmitt C, Armes SP. J Chem Soc Faraday Trans 1995;91:905.
[4] Armes SP, Vincent B. J Chem Soc Chem Commun 1987;288.
[5] Cawdery N, Obey TM, Vincent B. J Chem Soc Chem Commun 1988; 1189.
[6] Odegard R, Skotheim TA, Lee HS. J Electrochem Soc 1991;138(10): 2930.
[7] Armes SP, Aldissi M. Polymer 1990;31:569.
[8] Beadle PM, Rowan L, Mykytiuk J, Billingham NC, Armes SP. Polymer 1993;34:1561.
[9] Beaman M, Armes SP. Colloid Polym Sci 1993;271:70.
[10] Digar ML, Bhattacharyya SN, Mandal BM. Polymer 1994;35(2):377.
[11] Mandal TK, Mandal BM. Polymer 1995;36(9):1911.
[12] Mandal TK, Mandal BM. J Polym Sci Part A: Polym Chem 1999;37: 3723.
[13] Simmons MR, Chaloner PA, Armes SP. Langmuir 1995;11:4222.
[14] Qi Z, Pickup PG. Chem Mater 1997;9:2934.
[15] Gill M, Mykytiuk J, Armes SP, Edwards JL, Yeates T, Moreland PJ, Mollett C. J Chem Soc Chem Commun 1992;108.
[16] Gill M, Armes SP, Fairhurst D, Emmett SN, Pigott T, Idzorek GC. Langmuir 1992;8:2178.
[17] Maeda S, Armes SP. Chem Mater 1995;7:171.
[18] Biswas M, Ray SS, Liu Y. Synth Met 1999;105:99.
[19] Ray SS, Biswas M. Synth Met 2000;108:231.
[20] Beadle P, Armes SP, Gottesfeld S, Mombourquette C, Houlton R, Andrews WD, Agnew SF. Macromolecules 1992;25:2526.
[21] Liu CF, Maruyama T, Yamamoto T. Polym J 1993;25:363.
[22] Koopal CG, Feiters MC, Notle RJ, De Ruitter B, Schasfoort RB. Biosensors Bioelectronics 1992;7:461.
[23] Martin CR. Science 1994;266:1961.
[24] Martin CR. Chem Mater 1996;8:1739.
[25] Hulteen JC, Martin CR. J Mater Chem 1997;7:1075.
[26] Menon VP, Lei J, Martin CR. Chem Mater 1996;8:2382.
[27] Duchet J, Legras R, Demoustier-Champagne S. Synth Met 1998;98: 113.
[28] Demoustier-Champagne S, Ferain E, Legras R, Jerome C, Gerome R. Eur Polym J 1998;34:1767.
[29] Demoustier-Champagne S, Legras R. J Chim Phys PCB 1998;95: 1200.
[30] Demoustier-Champagne S, Stavaux PY. Chem Mater 1999;11:829.
[31] Jerome C, Demoustier-Champagne S, Legras R, Jerome R. Chem Eur J 2000;6(17):3089.
[32] Jerome C, Labaye DE, Bodart I, Jerome R. Synth Met 1999;101:3.
[33] Liu J, Wan M. J Polym Sci Part A: Polym Chem 2001;39:997.
[34] Huang J, Wan M. J Polym Sci Part A: Polym Chem 1999;37:151.
[35] Youging S, Wan M. J Polym Sci Part A: Polym Chem 1999;37:1443.
[36] Ricka J, Tanaka T. Macromolecules 1984;17:2916.
[37] Flory P, Erman B. Macromolecules 1982;15:800.
[38] Beltran S, Baker JP, Hooper HH, Blanch HW, Prausnitz JM. Macromolecules 1991;24:549.
[39] Kirsh Y, Janul NA, Popkov Y, Timashev SF. Zurnal fisicheskoj himiji 1999;73:2.
[40] Park TG, Hoffman AS. Macromolecules 1993;26:5045.
[41] Butterworth MD, Corradi R, Johal J, Lascelles SF, Maeda S, Armes SP. J Colloid Interface Sci 1995;174:510.
[42] Li H, Kumacheva E. Colloid Polym Sci 2003;281:1.
[43] Markham G, Obey TM, Vincent B. Colloid Surf 1990;51:239.